



Glioblastoma-specific anticancer activity of newly synthesized 3,5-disubstituted isoxazole and 1,4-disubstituted triazole-linked tyrosol conjugates

Imen Aissa^{a,1}, Zaineb Abdelkafi-Koubaa^{b,c,1}, Karim Chouaïb^a, Maroua Jalouli^d, Amine Assel^a, Anis Romdhane^a, Abdel Halim Harrath^d, Naziha Marrakchi^{b,c,e}, Hichem Ben Jannet^{a,*}

^a University of Monastir, Faculty of Science of Monastir, Laboratory of Heterocyclic, Chemistry, Natural Products and Reactivity, Team Medicinal Chemistry and Natural Products (LR11ES39), Department of Chemistry, Avenue of Environment, 5019 Monastir, Tunisia

^b Pasteur Institute of Tunis, LR20IPT01, Laboratory of Biomolecules, Venoms and Theranostic Applications, 1002 Tunis, Tunisia

^c University of Tunis El Manar, 1068 Tunis, Tunisia

^d King Saud University, Department of Zoology, College of Science, Riyadh, Saudi Arabia

^e University of Tunis El Manar, Faculty of Medicine of Tunis, 1068 Tunis, Tunisia

ARTICLE INFO

Keywords:

Tyrosol
Isoxazoles
Triazoles
Microwave-assisted synthesis
Antiproliferative activity

ABSTRACT

Two series of 3,5-disubstituted isoxazoles (**6a–e**) and 1,4-disubstituted triazoles (**8a–e**) derivatives have been synthesized from tyrosol (**1**), a natural phenolic compound, detected in several natural sources such as olive oil, and well-known by its wide spectrum of biological activities. Copper-catalyzed microwave-assisted 1,3-dipolar cycloaddition reactions between tyrosol-alkyne derivative **2** and two series of aryl nitrile oxides (**5a–e**) and azides (**7a–e**) regioselectively afforded 3,5-disubstituted isoxazoles (**6a–e**) and 1,4-triazole derivatives (**8a–e**), respectively in quantitative yields. Synthesized compounds were purified and characterized by spectroscopic means including 1D and 2D NMR techniques and HRMS analysis. The newly prepared hybrid molecules have been evaluated for their anticancer and hemolytic activities. Results showed that most derivatives displayed significant antiproliferative activity against human glioblastoma cancer cells (U87) in a dose-dependent manner. Compounds **6d** ($IC_{50} = 15.2 \pm 1.0 \mu\text{g/mL}$) and **8e** ($IC_{50} = 21.0 \pm 0.9 \mu\text{g/mL}$) exhibited more potent anticancer activity. Moreover, most derivatives displayed low hemolytic activity, even at higher concentrations which suggested that these classes of compounds are suitable candidates for further *in vivo* investigations. The obtained results allow us to consider the newly synthesized isoxazole- and triazole-linked tyrosol derivatives as promising scaffolds for the development of effective anticancer agents.

1. Introduction

Hybrid constructs from entities with known biological activity using “click” chemistry can be an important source for molecular diversity, making this a promising approach for the development of leads for medicinal chemistry applications [1,2]. Among these hybrids five membered heterocycles, such as 1,2,3-triazole/ isoxazole derivatives, have attracted special attention over the past decade and found wide applications in medicinal chemistry [3,4]. Isoxazoles have attracted considerable attention from organic and medicinal chemists due to their significant biological activities [4]. Successful applications of developing isoxazole compounds have resulted in multiple marketed drugs with diverse therapeutic activities such Sulfamethoxazole

(Antibacterial), Cycloserine (Antitubercular), Risperidone (Antipsychotic), Leflunomide (Antirheumatic) and Acivicin (Antitumor) [5]. In addition, more than thirty patents have been published describing the possible use of isoxazole compounds to treat several diseases, in particular cancer [4]. For example, Luminespib (resorcinylic isoxazole amide NVP-AUY922), an experimental anticancer drug candidate, is currently under 28 phase I/II clinical trials which most of them are completed [6]. It has shown promising activity in preclinical testing against several different tumor types by inhibiting the heat shock protein 90 (Hsp90), a chaperone protein that plays a role in the modification of a variety of proteins implicated in oncogenesis [7]. Others isoxazole derivatives showed an anticancer activity through apoptosis induction and cell cycle arrest [8–11].

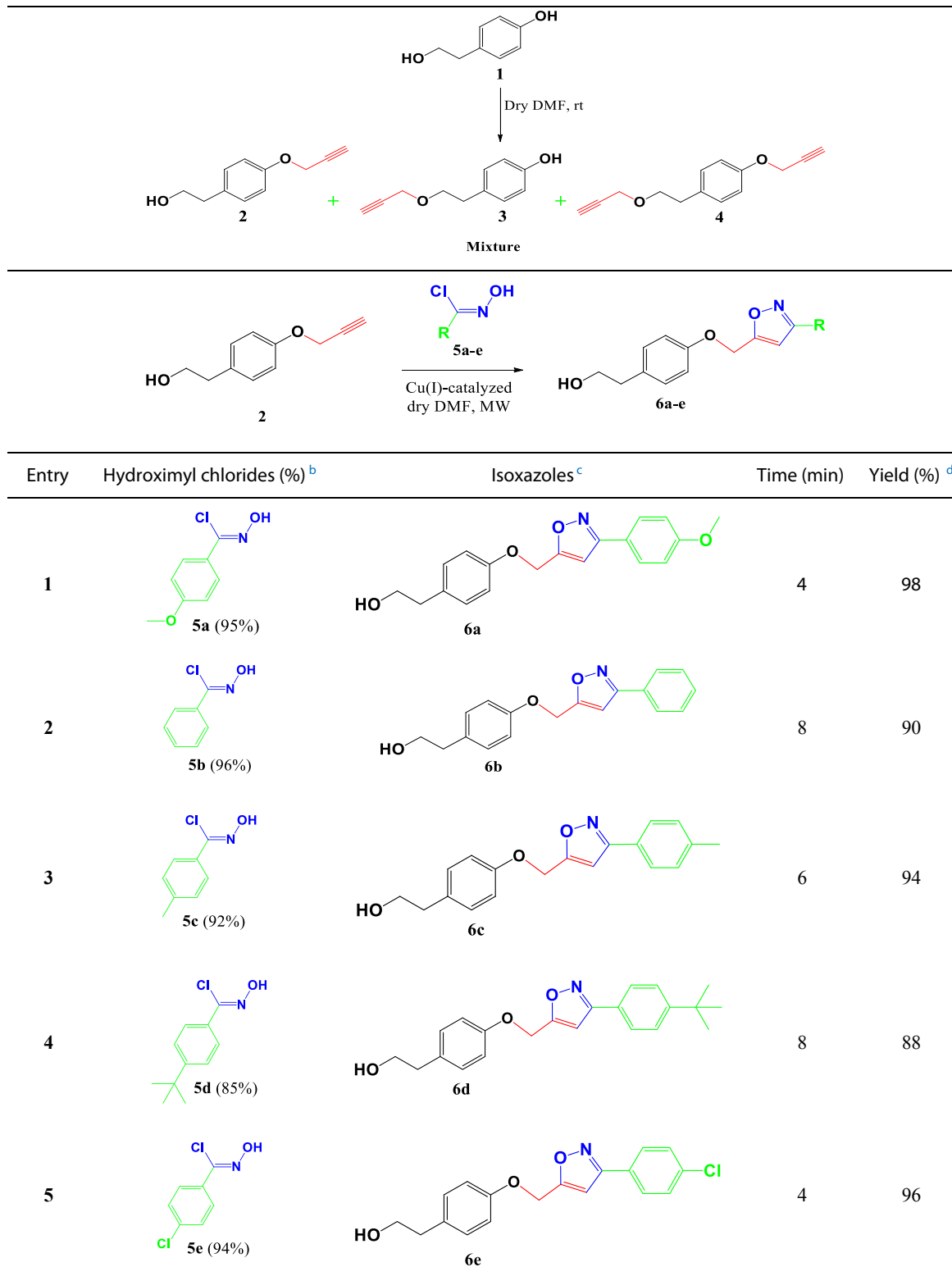
* Corresponding author.

E-mail address: hichem.bjannet@gmail.com (H. Ben Jannet).

¹ These authors contribute equally in this work.

On the other hand, triazoles are a class of *N*-heterocyclic compounds with great importance in medicinal chemistry based on their ability to act as pharmacophores and linkers between two or more substances of interest in molecular hybridization approaches [12]. These compounds exhibited an attractive wide range of targets biological potentials including anti-proliferative and anticancer against a panel of human cell lines [13–18]. Some of them, such as Cefatrizine and

Carboxyamidotriazole, have already been used in clinics or under clinical evaluation for cancer treatment [15]. Mechanistic exploration revealed that triazole derivatives induced apoptosis and cell cycle arrest [15,19]. Recently, several studies have reported that new triazole/isoxazole derivatives, with different pattern of substitution, exhibited significant anticancer activity against various malignant glioma cell lines including glioblastoma, the most malignant and invasive type of



Scheme 1. Synthesis of dipolarophiles 2–4^a and tyrosol-3,5-disubstituted isoxazoles (6a–e).

primary brain [20–22].

Interestingly, hybridization of 1,2,3-triazole / isoxazole with phenolic compounds has provided a new anticancer molecules [15]. A flavone/isoxazole fused heterocycles and flavone/1,2,3-triazole hybrid heterocycles compounds were synthesized *via* an intramolecular cyclization and Cu(I)-catalyzed click 1,3-dipolar cycloaddition and showed an antiproliferative activity against human breast cancer cell line [23]. Other 1,2,3-triazole-coumarin/flavone hybrids were synthesized and displayed potent anticancer activity against several human cell lines [24,25] *via* induction of apoptosis in cancer cells after accretion of reactive oxygen species (ROS) or reduction in mitochondrial membrane potential —[26,27]. Olive oil phenolic compounds are also an attractive moieties that could be important to drug design, given their wide variety of biological activities [28]. Among these compounds, the tyrosol (2-(4-hydroxyphenyl)-ethanol) (**1**), present also in wine [29], *Rhodiola rosea* [30], and marine fungi [31]. Tyrosol (**1**) and some of its derivatives have gained research interest due to their antiplatelet [32], antioxidant, anti-stress [33], anticancer [34] and antibacterial [35] activities. These data encourage to continue the hybridization of tyrosol with other pharmacophores such as 1,2,3-triazole / isoxazole moieties which may provide novel anticancer candidates.

In this study, we used tyrosol (**1**) as a starting material to synthesize new tyrosol-3,5-disubstituted isoxazoles (**6a–e**) *via* 1,3-dipolar cycloaddition using various aromatic hydroximyl chlorides, and access to 1,4-disubstituted triazole derivatives (**8a–e**) *via* CuAAC. Additionally, we developed a regioselective, simple, and versatile Cu(I)-catalyzed, microwave-assisted procedure for preparation of these series. Based on the above cited findings and the potential anticancer activity of isoxazoles and triazoles, the newly synthesized compounds have been evaluated for their antitumor effect against human glioblastoma cells (U87) as well as for their hemolytic activity.

2. Results and discussion

2.1. Chemistry

2.1.1. Synthesis of tyrosol-alkyne derivatives **2–4** as dipolarophiles

Tyrosol (**1**) was subjected to a propargylation in dry DMF at room temperature in the presence of NaH and propargyl bromide for 3 h. The reaction was monitored by TLC and yielded a mixture of differently propargylated compounds in a 97% global yield (Scheme 1). Chromatographic separation of this mixture over a silica-gel column afforded compounds **2** (76%), **3** (trace), and **4** (21%). The high yield of compound **2** relative to its analogues (**3** and **4**) was explained by the higher reactivity of the phenol function compared with alcohol.

The structures of the propargylated compounds **2–4** were unambiguously confirmed by their NMR and ESI-HRMS spectral data. The molecular formula of compound **2** (C₁₁H₁₂O₂) as determined by ESI-HRMS (*m/z* 177.0925 [M + H]⁺) agreed with a monopropargylated structure of tyrosol (**1**). Additionally, the molecular formula of compound **4** (C₁₄H₁₃O₂) as determined by ESI-HRMS (*m/z* 215.1080 [M + H]⁺) agreed with the dipropargylation of tyrosol (**1**). The position of the alkylation in the obtained derivatives was deduced by simple comparison of their NMR spectral data (¹H and ¹³C) with those of the starting substrate **1**. In addition to signals corresponding to the protons and carbons of tyrosol (**1**), new signals related to the alkyl group (methylene and methylidyne) were observed in NMR spectra (¹H and ¹³C).

The distinction between the structure of the propargylated derivative **2** compared to its analogue **3** was easily deduced by the relatively high deshielding of methylenic protons (δ_{H} 4.65, Fig. S1) of the propargyl moiety in **2** attached to the phenol function of **1** compared to the same protons (δ_{H} 4.15) in **3** (trace) where the propargyl moiety is attached to the primary alcohol function (Fig. S3). This deshielding is undoubtedly explained by the donor mesomeric effect + M exerted only by the non-binding doublets oxygen atom of the phenol function. Moreover, the NOESY spectrum of the cycloadduct **8c** (Fig. S21), taken as an example,

confirms the propargylation of the phenol function in **2** by the observation of an NOE between the methylenic protons (δ_{H} 5.25) of the propargyl fragment and the aromatic protons of tyrosol (δ_{H} 6.95, 2H, d, $J = 8.7$ Hz). The markedly high yield of **2** (76%) is explained by the relatively high acidity of the phenolic proton compared to that of the alcohol function, both of which react with the sodium hydride, to prepare *in situ* the nucleophilic entity which substitute the bromine atom in the propargyl bromide. We selected this quantitative dipolarophile **2** for use in 1,3-dipolar cycloaddition reactions.

2.1.2. Dipole synthesis

2.1.2.1. Preparation of hydroximyl chlorides (5a–e). Hydroximyl chlorides (**5a–e**) are key precursors essential for *in situ* generation of reactive nitrile oxides, which participate in 1,3-dipolar cycloaddition reactions for the synthesis of tyrosol-3,5-disubstituted isoxazoles. The precursors (**5a–e**) were already synthesized, in one of our previous works [2], from the appropriate aldehydes using a two-step reaction according to the general procedure described in the literature [36]. The desired aromatic imidoyl chlorides were obtained in yields ranging from 85% to 96% (Scheme 1). The intermediate nitrile oxide reagents were formed from *in situ* dehydrohalogenation of the corresponding hydroximyl chlorides (**5a–e**) using triethylamine as a base.

2.1.2.2. Preparation of aromatic azides (7a–e). The precursors (**7a–e**) were synthesized from the appropriate anilines using a two-step procedure involving diazotization with sodium nitrite under acidic conditions, followed by displacement with sodium azide [13]. The desired aromatic azides (**7a–e**) were obtained in high yields ranging from 90 to 98% (Scheme 2).

2.1.3. Synthesis of tyrosol-3,5-disubstituted isoxazoles (6a–e)

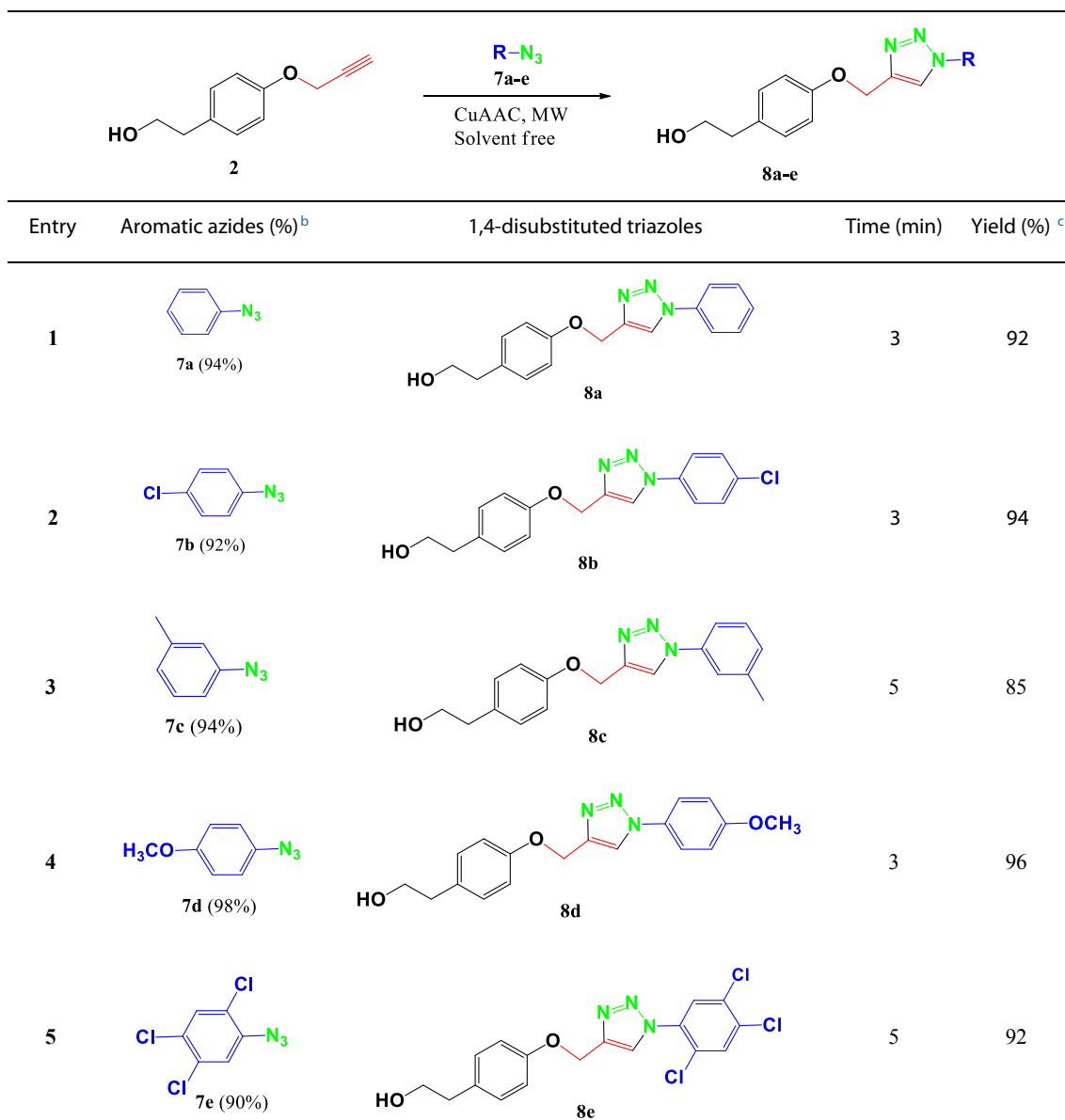
A regioselective approach was applied using dipolarophile **2** and various aromatic hydroximyl chlorides (**5a–e**) in the presence of CuI and Et₃N, resulting in the formation of regioselective tyrosol-3,5-disubstituted isoxazoles derivatives (**6a–e**) in excellent yields. All reactions were performed under microwave irradiation (200 W) and completed within 4 to 8 min. The new compounds (**6a–e**) were obtained in good yields (88–98%) (Scheme 1). This method has the advantage of being simple, regioselective, fast (shorter times than those of similar previous reactions [37]), and leading to high yields.

The synthesized tyrosol-3,5-disubstituted isoxazoles (**6a–e**) were characterized by ¹H, ¹³C NMR and ESI-HRMS analysis. The absence of the ¹H NMR signal relative to the terminal alkyne group in dipolarophile **2** at δ_{H} 2.51 (1H, t, $J = 2.4$ Hz) and the observation of a new signal at $\delta_{\text{H}} \sim 6.58$ – 6.65 (1H, s) corresponding to the C–H proton of the isoxazole ring supported the progress of the cycloaddition reaction to yield the desired 3,5-disubstituted isoxazoles **6a–e**. Their structures were also supported by their ¹³C NMR spectra, showing the disappearance of the terminal carbon signal of the alkyne group at $\delta_{\text{C}} \sim 75$ – 78 , and the appearance of a new signal relating to the tertiary carbon in the isoxazole ring at $\delta_{\text{C}} \sim 100$, 1–100.8.

2.1.4. CuAAC for the synthesis of tyrosol-1,4-disubstituted triazoles (8a–e)

A regioselective approach using a Huisgen 1,3-dipolar cycloaddition reaction (CuAAC) of alkyne **2** with various aromatic azides (**7a–e**) in the presence of CuI and Et₃N resulted in formation of regioselective 1,4-disubstituted triazoles derivatives (**8a–e**) in excellent yields (85–96%) (Scheme 2). All the reactions were performed under microwave irradiation (250 W) and achieved within 2 to 6 min under solvent-free conditions. The formed products were easily obtained from the reaction mixture by simple extraction [38].

The structures of the tyrosol-1,4-disubstituted triazoles regioisomers were established according to their spectral data. The ¹H NMR spectra of compounds **8a–e** showed a singlet at $\delta_{\text{H}} \sim 8.00$ – 8.08 attributable to the



Scheme 2. Tyrosol-1,4-disubstituted triazoles (8a–e) prepared by the CuAAC^a.

H-5 proton of the triazole ring, and signals were observed in the aromatic region (δ_{H} 6.90–7.80 attributable to the new aromatic protons introduced by the azides. These structures were further supported by ^{13}C NMR and DEPT spectra, which showed all of the expected carbon signals corresponding to the tyrosol-triazole derivatives, including the new aromatic carbons resonating at $\delta_{\text{C}} \sim 114.0$ – 160.0 introduced by the azides. The regioselectivity of this reaction leading exclusively to 1,4-regioisomers was supported by the dipolar interactions (NOE) observed between $\text{H}_{\text{5triazole}}/\text{H}_{\text{methylene}}$ and $\text{H}_{\text{5triazole}}/\text{H}_{\text{arom}}$, and the absence of any NOE between $\text{H}_{\text{methylene}}/\text{H}_{\text{arom}}$ [39,40]. HRMS data of all of the prepared derivatives were also in agreement with the proposed structures.

2.2. Pharmacological screening and/or biological evaluation

2.2.1. Antitumor activity

2.2.1.1. Antiproliferative activity. The antitumor potential of the newly synthesized compounds was evaluated against the human glioblastoma cell line (U87). Cells were incubated with different concentrations of

tyrosol (1) and its derivatives (6a–e) and (8a–e) for 24 and 72 h. Compared with natural tyrosol (1), all of the synthesized compounds decreased U87 cell viability in a dose and time-dependent manners (Figs. 1, 2). Interestingly, tyrosol-coupled 3,5-disubstituted isoxazole derivatives (6a–e) ($\text{IC}_{50} = 52$ – $80 \mu\text{g/mL}$) (Fig. 1A) were more active towards U87 cells than tyrosol-coupled 1,4-disubstituted triazoles (8a–e) ($\text{IC}_{50} > 100 \mu\text{g/mL}$, except for 8e) after 24 h treatment (Fig. 1B). These findings suggested that changing substitutions in the aromatic system and differences in triazole or isoxazole rings influenced the cytotoxic activity against glioblastoma cells.

When the treatment was extended for 72 h, all derivatives at increasing concentrations (0– $100 \mu\text{g/mL}$) exerted potent antiproliferative activity against U87 cells (Fig. 2). Moreover, the results showed that the junction of tyrosol (1) with isoxazoles (6a–e) (Fig. 2A) and triazoles (8a–e) (Fig. 2B) through the linker methylene improved its antiproliferative activity at lower concentrations. Additionally, tyrosol-coupled 3,5-disubstituted isoxazole derivatives (6a–e) ($\text{IC}_{50} = 15$ – $31 \mu\text{g/mL}$) exhibited a higher degree of growth inhibition against U87 cells than tyrosol-coupled 1,4-disubstituted triazoles (8a–e) ($\text{IC}_{50} > 30 \mu\text{g/mL}$, except for 8e) (Table 1).

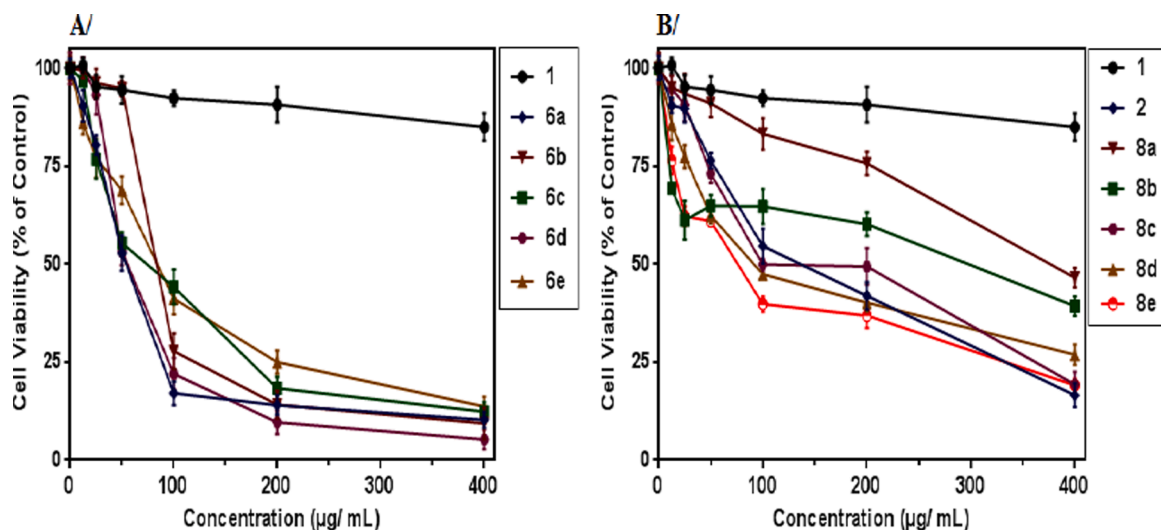


Fig. 1. Tyrosol derivatives affect U87 cell viability. (A) U87 cells treated with tyrosol (1) and the synthesized isoxazoles (6a–e). (B) Cells treated with tyrosol (1), tyrosol-alkyne 2, and the synthesized triazoles (8a–e). Cells were treated with increasing concentrations for 24 h, and their viability was determined by metabolic rate using the MTT assay. Absorbance values were measured at 560 nm and normalized against untreated cells. Data represent the mean \pm SEM of three independent experiments performed in triplicate. All the data were statistically significant ($p < 0.05$) except tyrosol (1) (at 12.5 and 25 $\mu\text{g}/\text{mL}$) and 6b, 6c, 6d and 8a at 12.5 $\mu\text{g}/\text{mL}$. MTT, 3,4,5-dimethylthiazol-2-yl, 2,5 diphenyltetrazolium bromide; SEM, standard error of the mean.

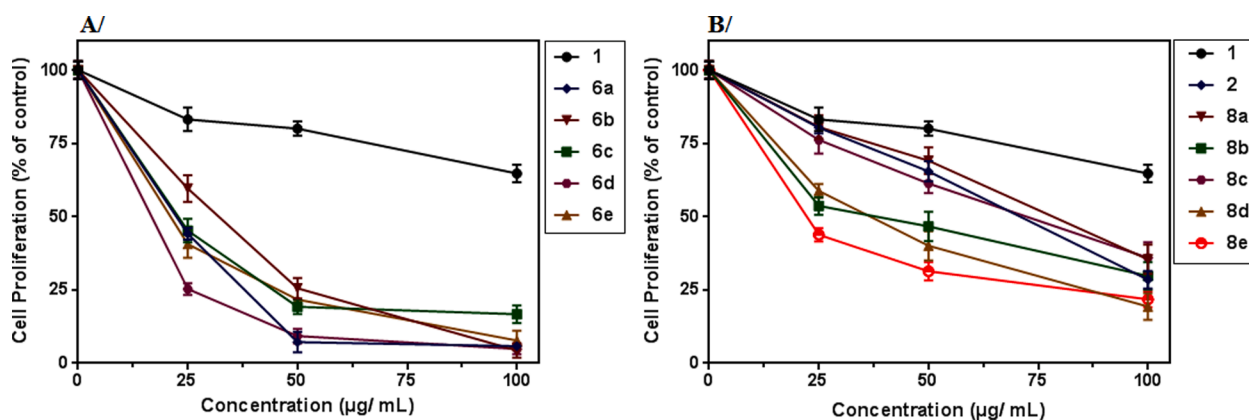


Fig. 2. Effect of tyrosol (1) and its derivatives on U87 cell proliferation. (A) U87 cells treated with tyrosol (1) and the synthesized isoxazoles (6a–e) for 72 h. (B) U87 cells treated with tyrosol (1), tyrosol-alkyne 2, and the synthesized triazoles (8a–e) at various concentrations for 72 h. Data represent the mean \pm SEM of three independent experiments performed in triplicate. All the data were statistically significant $p < 0.05$. SEM, standard error of the mean.

Table 1

IC₅₀ Values ($\mu\text{g}/\text{mL}$ and μM) of compounds 1, (6a–e) and (8a–e) against U87 tumor cell proliferation.

Compounds	1	6a	6b	6c	6d	6e	3	8a	8b	8c	8d	8e	Temozolomide
IC ₅₀ ($\mu\text{g}/\text{mL}$)	>100	22.1 \pm 0.5	31.0 \pm 0.9	22.5 \pm 0.8	15.2 \pm 1.0	20.3 \pm 0.4	72.1 \pm 0.8	78.0 \pm 1.2	30.0 \pm 0.5	72.3 \pm 0.2	34.2 \pm 0.8	21.0 \pm 0.9	–
IC ₅₀ (μM)	>400	67.6 \pm 1.5	104.5 \pm 3.0	72.4 \pm 2.5	42.8 \pm 2.8	61.4 \pm 1.2	406.4 \pm 4.5	263.4 \pm 4.0	90.8 \pm 1.5	233.1 \pm 0.6	104.8 \pm 2.3	52.7 \pm 2.2	53.85[42]

For the 3,5-disubstituted isoxazole (6a–e) derivatives, compounds 6a (4-OCH₃), 6d (4-*t*-Bu), and 6e (4-Cl) displayed the highest antiproliferative activity towards U87 cells, with IC₅₀ values of 22.1 $\mu\text{g}/\text{mL}$ (67.6 μM), 15.2 $\mu\text{g}/\text{mL}$ (42.8 μM) and 20.3 $\mu\text{g}/\text{mL}$ (61.4 μM), respectively. Previous studies reported the antiproliferative activity of isoxazole derivatives against human glioblastoma cell lines [22,41]. In the series of the 1,4-disubstituted triazole derivatives (8a–e), compounds 8b (4-Cl) and 8e (2,4,5-trichlo) exhibited the most potent antiproliferative activity against U87 cells, with IC₅₀ values of 30.0 $\mu\text{g}/\text{mL}$ (90.8 μM) and 21.0 $\mu\text{g}/\text{mL}$ (52.7 μM), respectively. In agreement with our results, it has been shown that 1,4-disubstituted-1,2,3-triazole derivatives exhibited

antitumor potential against U87, GBM02 and GBM95 cell lines with IC₅₀ values ranging from \sim 20 to 190 μM for 72 h treatments [20].

Interestingly, all these isoxazole and triazole derivatives exhibits higher antiproliferative activity than Temozolomide (Table 1), the most widely used chemotherapy for patients with glioblastoma [42].

Given this activity profile, we generated a structure–activity relationship showing that compounds with methyl, methoxy, or chlorine substitution at R groups in isoxazole derivatives and compounds with a chlorine substitution at R groups in triazole derivatives were more effective against U87 cells. Furthermore, we observed that the presence of more than one methyl group or chlorine atom (three in these cases)

played a significant role in enhancing the antiproliferative activity. In the present study, a benzene ring substituted at three positions (**8e**) resulted in higher activity than the derivative with a benzene ring substituted only at a *para*-position (**8b**).

2.2.1.2. Analysis of cell morphology. To investigate the effect of tyrosol derivatives on U87 cells, we examined changes in cell morphology (Fig. 3). After 72 h and compared with controls, treated U87 cells with isoxazole (Fig. 3A) and triazole (Fig. 3B) derivatives exhibited decreased cell density and morphological changes, such as acquisition of round shape, shrinkage and spherical cellular protrusions. These abnormal morphological characteristics provided insight into the anticancer effect of these compounds.

2.2.1.3. Pro-apoptotic activity on U87 cells. Based on the promising antiproliferative effect against U87 cells, compounds **6a**, **6d**, **8b**, and **8e** were chosen for deeper evaluations aimed at better understanding its mechanism of action. These compounds were evaluated for a possible pro-apoptotic effect determined by Annexin V / PI assay. U87 cells were treated with **6a**, **6d**, **8b** (4-Cl), or **8e** (2,4,5-trichlo) at their respective IC₅₀ values (22.1, 15.2, 30.0, and 21.0 µg/mL) for 72 h. Among the four tested compounds, all were found to possess the ability to induce apoptosis on U87 cells (percentage of apoptotic cells = 56%, 20%, 47%, and 53%, respectively) (Fig. 4). These results suggested that the newly synthesized compounds exerted its anticancer activity through the induction of apoptosis in U87 cells. As it has been shown previously, several triazole/ isoxazole derivatives trigger antiproliferative effects through the induction of apoptosis. For example, anticancer isoxazole derivatives have been shown to activate apoptotic pathways in U251-MG and T98G glioma cell lines [22]. In addition to this, a pyrazolo [3,4-*d*]pyrimidin-4(5*H*)-ones tethered to 1,2,3-triazoles compound exhibited significant anti-proliferative and pro apoptotic effect on glioma cells (U87) by the cleavage of Caspase-3, PARP and up regulation of p53 [43]. Further investigation should be conducted in order to fully elucidate the pro-apoptotic activity.

2.2.2. Hemolytic activity

The promising anticancer activity shown by the synthetic compounds demanded further safety analysis. In fact, hemolytic activity is a major limitation on the development of chemical compounds as pharmaceutical agents. Indeed, numerous therapeutic compounds do not enter the clinical trials due to their high hemolytic activity [44]. Therefore, the hemocompatibility evaluation of the tyrosol derivatives

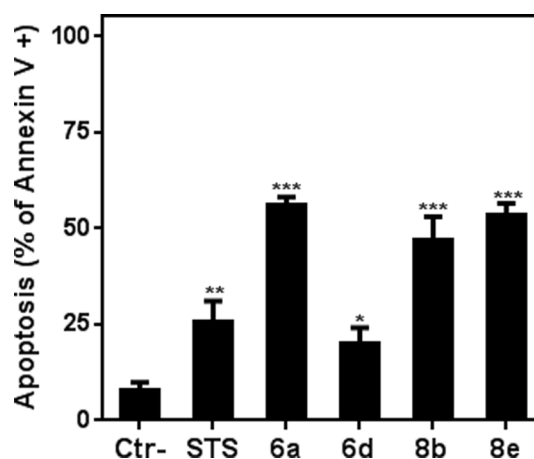


Fig. 4. Apoptosis induction in U87 cells treated with **6a**, **6d**, **8b**, and **8e** for 72 h according to Annexin-V and PI staining. Cells treated with 0.5 µM Staurosporine were used as positive control and untreated cells as negative control. Data represent the mean ± SEM of two independent experiments. The values of $p < 0.05$, $p < 0.01$ and $p < 0.001$ were considered as statistically significant (*), very significant (**), highly significant difference (***) respectively, unless otherwise mentioned. PI, propidium iodide; SEM, standard error of the mean.

was performed using hemolytic test on human erythrocytes (Fig. 5). All of the isoxazole (Fig. 5A) and triazole (Fig. 5B) compounds induced < 10% hemolysis, even at a higher concentration of 400 µg/mL, except **6d** (this compound bearing an *isopropyl* group in its isoxazole moiety induced ~ 40% hemolysis at 400 µg/mL). These data indicated that the triazole and isoxazole derivatives did not induce red blood membrane damage and hemoglobin release. This result reinforced the potential of these compounds for future *in vivo* investigations as a new anticancer prototype. These finding provide a new insight for designing novel anticancer agents with low hemolytic activity.

3. Conclusion

In summary, we synthesized novel 3,5-disubstitued isoxazole and 1,4-disubstitued triazole tyrosol conjugates (**6a-e**) and (**8a-e**), respectively using microwave irradiation. The synthesized derivatives exhibited higher antiproliferative activities towards human glioblastoma cells (U87) with slight hemolytic activity relative to the parent tyrosol. Among the tested compounds, **6d** and **8e** exhibited the highest

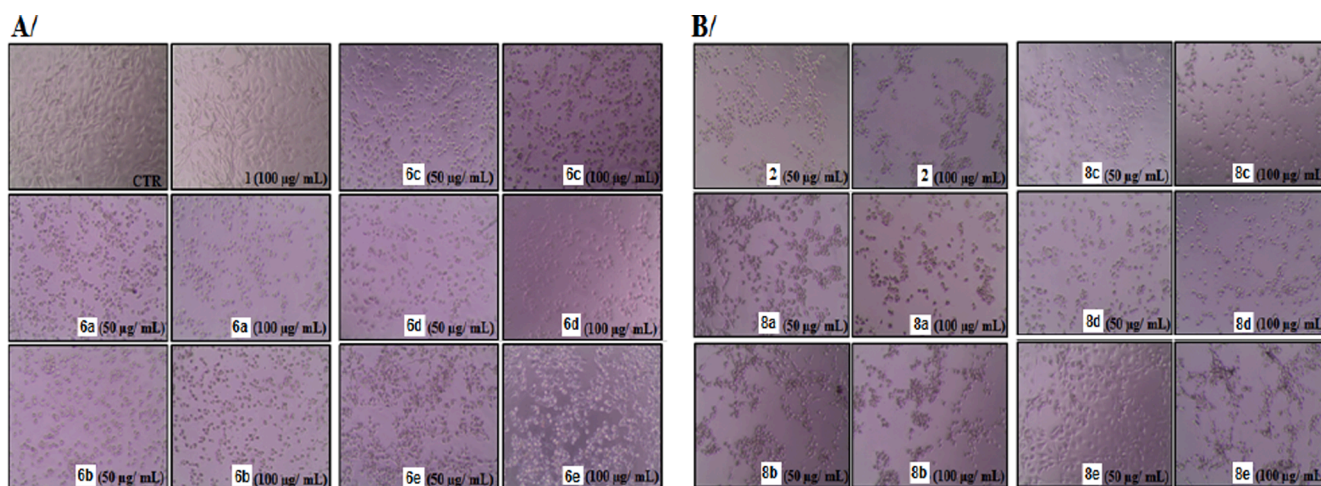


Fig. 3. Morphological changes of U87 cells treated with (A) tyrosol (**1**) and its derivatives (**6a-e**) or (B) tyrosol (**1**), tyrosol-alkyne **2**, and its derivatives (**8a-e**). Morphological differences were observed by inverted phase-contrast microscopy (magnification: 10 ×) after treatment with chemical compounds (50 µg/mL or 100 µg/mL) for 72 h. Untreated cells were used as controls.

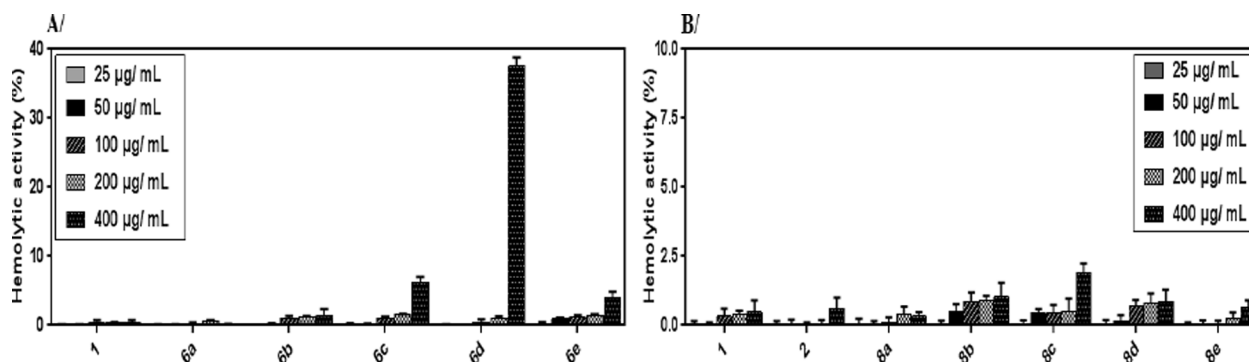


Fig. 5. Hemolytic activity of tyrosol (1) and its derivatives on human erythrocytes at different concentrations. (A) Hemolytic activity of tyrosol (1) and its derivatives (6a–e). (B) Hemolytic activity of tyrosol (1), tyrosol-alkyne 2, and its derivatives (8a–e). Data are presented as a percentage of hemolysis relative to a positive control (100%; 1% Triton X-100). Data represent the mean \pm SEM of independent assays performed in triplicate. SEM, standard error of the mean.

selective antiproliferative effect. Preliminary results from the Annexin-V assay indicate that these compounds induced apoptosis in human glioblastoma cancer cell line U87. Future studies are necessary to identify and validate a potential lead compound, as well as elucidate the mechanism underlying the anticancer effect.

4. Materials and methods

4.1. General experimental procedures

Tyrosol (1) was purchased from Fluka (Bucha, Switzerland). Solvents were distilled and dried using standard methods. Melting points were determined on a Büchi 510 apparatus using capillary tubes. Commercial thin-layer chromatography (TLC) plates (silica gel 60; F₂₅₄) were used to monitor the progress of the reactions. Column chromatography was performed with silica gel 60 (particle size: 40–63 µm). High-resolution mass spectrometry (HRMS) was performed using an LCT Premier XE system [electrospray ionization (ESI) technique, positive mode; Waters, Milford, MA, USA]. For ESI experiments, leucine-enkephaline peptide was employed as the LockSpray lock mass. ¹H (300 MHz; 16–32 scans) and BB-decoupled ¹³C (75 MHz; 256–2048 scans) nuclear magnetic resonance (NMR) spectra were recorded at room temperature on an AM-300 Fourier transform spectrometer (Bruker Daltonik, Bremen, Germany) equipped with a 10-mm probe in deuterated chloroform with all chemical shifts (δ) and reported in ppm (non-deuterated solvent was used as a control standard). Coupling constants were measured in Hz, with signals denoted, as follows: s, singlet; d, doublet; t, triplet; and m, multiplet.

Cell culture medium [minimum essential medium Eagle (MEM)], trypsin-EDTA, phosphate buffer saline (PBS), fetal bovine serum (FBS), penicillin and streptomycin mixture, and L-glutamine (200 mM) were purchased from GIBCO-BRL (Paisley, UK). Dimethyl sulfoxide (DMSO) and 3,4,5-dimethylthiazol-2-yl, 2,5 diphenyltetrazolium bromide (MTT) were purchased from Sigma (Saint Quentin Fallavier, France). All other reagents were of analytical grade.

4.2. Chemistry

4.2.1. General procedure for the synthesis of tyrosol-alkyne derivatives 2–4

To a solution of tyrosol (1) (2 g; 14.5 mmol) in dry *N,N*-dimethylformamide (DMF; 4 mL), sodium hydride (29 mmol) and propargyl bromide (43.5 mmol) were added, and the reaction mixture was stirred at room temperature for 3 h, with the reaction monitored by TLC. After reaction completion, the residue was diluted with water (200 mL), and the mixture was extracted with ethyl acetate (3 \times 100 mL). The combined organic layer was dried over anhydrous sodium sulfate and evaporated to dryness, followed by purification over a silica gel column and elution with petroleum ether/ethyl acetate (6:4 then 1:1) to obtain

the alkyl derivatives 2 (76%), 3 (trace), and 4 (21%).

4.2.1.1. 2-(4-Propargyloxyphenyl)-ethanol (2). White solid; mp: 112–114 °C; ¹H NMR (300 MHz, CDCl₃): δ 7.14 (2H, d, *J* = 8.7 Hz), 6.91 (2H, d, *J* = 8.7 Hz), 4.65 (2H, d, *J* = 2.1 Hz), 3.77 (2H, t, *J* = 6.6 Hz), 2.78 (2H, t, *J* = 6.6 Hz), 2.51 (1H, t, *J* = 2.4 Hz), 2.06 (1H, s); ¹³C NMR (75 MHz, CDCl₃): δ 155.7, 131.1, 129.5, 114.5, 78.2, 75.0, 63.1, 55.4, 37.8; HRMS (ESI⁺): calcd. for (C₁₁H₁₃O₂)⁺ [M + H]⁺ 177.0924, found 177.0925.

4.2.1.2. 1-(propargyloxy)-4-(propargyloxyethyl)-benzene (4). White solid; mp: 105–107 °C; ¹H NMR (300 MHz, CDCl₃): δ 7.16 (2H, d, *J* = 8.4 Hz), 6.91 (2H, d, *J* = 8.4 Hz), 4.66 (2H, d, *J* = 2.4 Hz), 4.15 (2H, d, *J* = 2.4 Hz), 3.72 (2H, t, *J* = 7.2 Hz), 2.87 (2H, t, *J* = 6.9 Hz), 2.50 (1H, t, *J* = 2.1 Hz), 2.41 (1H, t, *J* = 2.4 Hz); ¹³C NMR (75 MHz, CDCl₃): δ 155.6, 131.2, 129.3, 114.4, 79.3, 78.2, 74.8, 73.8, 70.5, 57.6, 55.3, 34.6; HRMS (ESI⁺): calcd. for (C₁₄H₁₅O₂)⁺ [M + H]⁺ 215.1081, found 215.1080.

4.2.2. General procedure for the synthesis of 3,5-disubstituted isoxazoles (6a–e)

To a mixture of selected alkyne 2 (0.102 g; 0.57 mmol), triethylamine (1.14 mmol), and 0.1 equiv. Cu(I) iodide (CuI) in dry DMF, the appropriate hydroxymyl chlorides 5 (2 equiv.) were added at room temperature with stirring, after which the mixture was subjected to microwave irradiation at 200 W for 4 to 8 min. The crude mixture was then diluted with water, extracted with ethyl acetate (3 \times 40 mL), and the organic layer was dried over anhydrous Na₂SO₄. After removal of solvent *in vacuo*, the resulting residue was purified by silica gel column chromatography and eluted with petroleum ether/ethyl acetate (1:1) to obtain the new 3,5-disubstituted isoxazoles (6a–e) in 88% to 98% yields.

4.2.2.1. 2-(4-((3-(4-methoxyphenyl)isoxazol-5-yl)methoxy)phenyl)ethanol (6a). Yellowish solid; mp: 101–103 °C; ¹H NMR (300 MHz, CDCl₃): δ 7.79 (2H, d, *J* = 6.3 Hz), 7.75 (2H, d, *J* = 6.6 Hz), 7.21 (2H, d, *J* = 6.6 Hz), 6.94 (2H, d, *J* = 6.6 Hz), 6.58 (1H, s), 5.17 (2H, s), 3.94 (3H, s), 3.85 (2H, t, *J* = 6.9 Hz), 2.84 (2H, t, *J* = 6.9 Hz); ¹³C NMR (75 MHz, CDCl₃): δ 168.3, 161.6, 160.6, 156.0, 131.5, 131.4, 129.6, 128.2, 127.7, 126.2, 125.5, 114.6, 114.5, 100.5, 63.1, 61.1, 55.7, 37.7; HRMS (ESI⁺): calcd. for (C₁₉H₂₀NO₄)⁺ [M + H]⁺ 326.1401, found 326.1392.

4.2.2.2. 2-(4-((3-phenylisoxazol-5-yl)methoxy)phenyl)ethanol (6b). White solid; mp: 100–102 °C; ¹H NMR (300 MHz, CDCl₃): δ 7.83 (2H, m), 7.47 (3H, m), 7.18 (2H, d, *J* = 6.6 Hz), 6.97 (2H, d, *J* = 6.6 Hz), 6.65 (1H, s), 5.20 (2H, s), 3.85 (2H, t, *J* = 6.6 Hz), 2.84 (2H, t, *J* = 6.6 Hz); ¹³C NMR (75 MHz, CDCl₃): δ 168.1, 162.0, 156.1, 131.5, 129.6, 129.5, 128.4, 128.3, 126.3, 114.5, 100.1, 63.1, 61.1, 37.8; HRMS (ESI⁺): calcd. for (C₁₈H₁₈NO₃)⁺ [M + H]⁺ 296.1295, found 296.1299.

4.2.2.3. 2-(4-((3-(*p*-tolyl)isoxazol-5-yl)methoxy)phenyl)ethanol (6c). White solid; mp: 107–109 °C; $^1\text{H NMR}$ (300 MHz, CDCl_3): δ 7.71 (2H, d, $J = 6.9$ Hz), 7.27 (2H, d, $J = 6.6$ Hz), 7.19 (2H, d, $J = 6.6$ Hz), 6.96 (2H, d, $J = 6.6$ Hz), 6.62 (1H, s), 5.20 (2H, s), 3.85 (2H, t, $J = 6.9$ Hz), 2.84 (2H, t, $J = 6.9$ Hz), 2.42 (3H, s); $^{13}\text{C NMR}$ (75 MHz, CDCl_3): δ 167.9, 161.9, 156.1, 139.7, 131.4, 129.6, 129.4, 129.1, 126.2, 125.5, 114.6, 114.5, 100.7, 63.1, 61.1, 37.7, 20.8; HRMS (ESI^+): calcd. for $(\text{C}_{19}\text{H}_{20}\text{NO}_3)^+ [\text{M} + \text{H}]^+$ 310.1452, found 310.1435.

4.2.2.4. 2-(4-((3-(4-(*tert*-butyl)phenyl)isoxazol-5-yl)methoxy)phenyl)ethanol (6d). White solid; mp: 98–100 °C; $^1\text{H NMR}$ (300 MHz, CDCl_3): δ 7.72 (2H, d, $J = 8.7$ Hz), 7.46 (2H, d, $J = 8.4$ Hz), 7.15 (2H, d, $J = 5.4$ Hz), 6.93 (2H, d, $J = 6.6$ Hz), 6.60 (1H, s), 5.16 (2H, s), 3.81 (2H, t, $J = 6.3$ Hz), 2.80 (2H, t, $J = 6.3$ Hz), 1.34 (9H, s); $^{13}\text{C NMR}$ (75 MHz, CDCl_3): δ 167.9, 161.9, 156.1, 152.9, 131.4, 131.0, 129.6, 129.4, 129.1, 126.2, 125.4, 114.6, 114.5, 100.8, 63.1, 61.1, 37.8, 34.3, 30.6; HRMS (ESI^+): calcd. for $(\text{C}_{22}\text{H}_{26}\text{NO}_3)^+ [\text{M} + \text{H}]^+$ 352.1921, found 352.1922.

4.2.2.5. 2-(4-((3-(4-chlorophenyl)isoxazol-5-yl)methoxy)phenyl)ethanol (6e). Yellow paste; mp: 112–114 °C; $^1\text{H NMR}$ (300 MHz, CDCl_3): δ 7.72 (2H, dd, $J = 6.9$; 2.1 Hz), 7.41 (2H, dd, $J = 6.9$; 2.1 Hz), 7.15 (2H, dd, $J = 6.6$; 2.1 Hz), 6.91 (2H, dd, $J = 6.6$; 2.1 Hz), 6.59 (1H, s), 5.16 (2H, s), 3.81 (2H, t, $J = 6.3$ Hz), 2.80 (2H, t, $J = 6.3$ Hz); $^{13}\text{C NMR}$ (75 MHz, CDCl_3): δ 168.5, 161.0, 156.0, 135.7, 131.6, 129.6, 129.4, 129.0, 127.6, 126.8, 114.6, 114.5, 100.6, 63.1, 61.1, 37.7; HRMS (ESI^+): calcd. for $(\text{C}_{18}\text{H}_{17}\text{ClNO}_3)^+ [\text{M} + \text{H}]^+$ 330.0906, found 330.0886.

4.2.3. General procedure for synthesizing tyrosol-1,4-disubstituted triazoles (8a–e): CuAAC

Under solvent-free conditions, 0.102 g (0.57 mmol) of dipolarophile (**2**), CuI (0.5 equiv.), and triethylamine (1 equiv.) were mixed at room temperature, followed by the addition of aryl-azide **7** (1.14 mmol) and exposure to microwave irradiation at 250 W for 2 to 6 min. The crude mixture was then extracted with ethyl acetate (3 \times 35 mL), and the combined organic layer was dried over anhydrous sodium sulfate, concentrated under reduced pressure, and purified by column chromatography using a petroleum ether and ethyl acetate mixture as eluents to obtain pure (**8a–e**) in 85% to 98% yields.

4.2.3.1. 2-(4-((1-phenyl-1H-1,2,3-triazol-4-yl)methoxy)phenyl)ethanol (8a). White solid; mp: 120–122 °C; $^1\text{H NMR}$ (300 MHz, CDCl_3): δ 8.06 (1H, s), 7.73 (2H, d, $J = 7.5$ Hz), 7.49 (3H, m), 7.16 (2H, d, $J = 8.4$ Hz), 6.98 (2H, d, $J = 8.4$ Hz), 5.28 (2H, s), 3.83 (2H, t, $J = 6.6$ Hz), 2.82 (2H, t, $J = 6.6$ Hz); $^{13}\text{C NMR}$ (75 MHz, CDCl_3): δ 156.4, 144.5, 136.4, 130.8, 129.6, 129.2, 128.3, 120.4, 120.1, 114.4, 63.2, 61.6, 37.8; HRMS (ESI^+): calcd. for $(\text{C}_{17}\text{H}_{18}\text{N}_3\text{O}_2)^+ [\text{M} + \text{H}]^+$ 296.1408, found 296.1381.

4.2.3.2. 2-(4-((1-(4-chlorophenyl)-1H-1,2,3-triazol-4-yl)methoxy)phenyl)ethanol (8b). Dark red solid; mp: 116–118 °C; $^1\text{H NMR}$ (300 MHz, CDCl_3): δ 8.01 (1H, s), 7.67 (2H, d, $J = 7.2$ Hz), 7.48 (2H, d, $J = 7.5$ Hz), 7.16 (2H, d, $J = 8.7$ Hz), 6.98 (2H, d, $J = 8.7$ Hz), 5.26 (2H, s), 3.82 (2H, t, $J = 6.3$ Hz), 2.81 (2H, t, $J = 6.6$ Hz); $^{13}\text{C NMR}$ (75 MHz, CDCl_3): δ 156.3, 144.9, 134.9, 134.2, 130.9, 129.6, 129.4, 121.2, 120.2, 114.5, 63.1, 61.6, 37.8; HRMS (ESI^+): calcd. for $(\text{C}_{17}\text{H}_{17}\text{ClN}_3\text{O}_2)^+ [\text{M} + \text{H}]^+$ 330.1018, found 330.1018.

4.2.3.3. 2-(4-((1-(*m*-tolyl)-1H-1,2,3-triazol-4-yl)methoxy)phenyl)ethanol (8c). White solid; mp: 112–114 °C; $^1\text{H NMR}$ (300 MHz, CDCl_3): δ 8.01 (1H, s), 7.55 (1H, s), 7.49 (1H, d, $J = 8.1$ Hz), 7.37 (1H, t, $J = 7.8$ Hz), 7.23 (1H, d, $J = 7.8$ Hz), 7.15 (2H, d, $J = 8.7$ Hz), 6.95 (2H, d, $J = 8.7$ Hz), 5.25 (2H, s), 3.81 (2H, t, $J = 6.6$ Hz), 2.80 (2H, t, $J = 6.6$ Hz), 2.43 (3H, s); $^{13}\text{C NMR}$ (75 MHz, CDCl_3): δ 156.4, 144.4, 139.5, 136.4, 130.8, 129.5, 129.1, 129.0, 120.7, 120.4, 117.1, 114.4, 63.1, 61.7, 37.8, 20.8; HRMS (ESI^+): calcd. for $(\text{C}_{18}\text{H}_{20}\text{N}_3\text{O}_2)^+ [\text{M} + \text{H}]^+$ 310.1564, found 310.1550.

4.2.3.4. 2-(4-((1-(4-methoxyphenyl)-1H-1,2,3-triazol-4-yl)methoxy)phenyl)ethanol (8d). White solid; mp: 117–119 °C; $^1\text{H NMR}$ (300 MHz, CDCl_3): δ 8.00 (1H, s), 7.63 (2H, d, $J = 8.9$ Hz), 7.17 (2H, d, $J = 8.5$ Hz), 7.02 (2H, d, $J = 8.9$ Hz), 6.97 (2H, d, $J = 8.5$ Hz), 5.26 (2H, s), 3.87 (3H, s), 3.83 (2H, t, $J = 6.6$ Hz), 2.82 (2H, t, $J = 6.6$ Hz); $^{13}\text{C NMR}$ (75 MHz, CDCl_3): δ 159.9, 156.9, 144.8, 131.4, 130.4, 130.1, 122.2, 121.1, 114.9, 114.8, 63.7, 62.1, 55.6, 38.3; HRMS (ESI^+): calcd. for $(\text{C}_{18}\text{H}_{20}\text{N}_3\text{O}_3)^+ [\text{M} + \text{H}]^+$ 326.1513, found 326.1523.

4.2.3.5. 2-(4-((1-(2,4,5-trichlorophenyl)-1H-1,2,3-triazol-4-yl)methoxy)phenyl)ethanol (8e). White solid; mp: 111–113 °C; $^1\text{H NMR}$ (300 MHz, CDCl_3): δ 8.05 (1H, s), 7.76 (1H, s), 7.68 (1H, s), 7.13 (2H, d, $J = 8.4$ Hz), 6.93 (2H, d, $J = 8.4$ Hz), 5.25 (2H, s), 3.80 (2H, t, $J = 6.3$ Hz), 2.79 (2H, t, $J = 6.6$ Hz); $^{13}\text{C NMR}$ (75 MHz, CDCl_3): δ 156.2, 144.1, 139.5, 134.3, 133.3, 131.9, 131.0, 129.5, 129.4, 128.3, 126.6, 124.0, 115.0, 114.5, 63.2, 61.5, 37.7; HRMS (ESI^+): calcd. for $(\text{C}_{17}\text{H}_{15}\text{Cl}_3\text{N}_3\text{O}_2)^+ [\text{M} + \text{H}]^+$ 398.0239, found 398.0229.

4.3. Biological assay

4.3.1. Anticancer activity

4.3.1.1. Cell line and cell culture conditions. Human glioblastoma cell line (U87 cells) was cultured in MEM medium supplemented with 10% fetal bovine serum, L-glutamine and 100 IU of penicillin/ streptomycin in a humidified environment with 5% CO_2 at 37 °C.

4.3.1.2. Cytotoxic and antiproliferative assays. The anticancer activity of tyrosol (**1**) and its novel derivatives on U87 cell viability and proliferation was evaluated using an MTT assay [45]. The MTT assay evaluates cell metabolism based on the ability of mitochondrial succinate dehydrogenase to convert the yellow compound MTT to a blue formazan dye. The amount of dye produced is proportional to the number of live metabolically active cells. U87 cells at optimal density were seeded into 96-well microplates (Nunc microplates; Thermo Fisher Scientific, Waltham, MA, USA) and incubated overnight to allow attachment. Tyrosol (**1**) and its derivatives were serially diluted and added to the wells to their final respective concentrations and incubated for 24 h or 72 h. Additionally, morphological changes in the treated cells were examined and recorded under an inverted phase-contrast microscope (Leica, Mannheim, Germany). After incubation with different concentrations of compounds, MTT solution (500 $\mu\text{g}/\text{mL}$) was added and the cells were incubated for another 4 h. DMSO (100 μL) was then added to dissolve the formed violet formazan crystals within metabolically viable cells. Absorbance was determined by a microplate reader at 560 nm, and the results were expressed as a percentage of cell viability. Cells incubated with only medium were used as controls representing 100% viability or proliferation. Temozolomide was employed as a positive control [42], and all assays were performed in triplicate.

4.3.1.3. Flow cytometric analysis of apoptosis. Briefly, U87 cells were treated with **6a**, **6d**, **8b** and **8e** at their respective 50% inhibitory concentration (IC_{50}) values. After 72 h, all cell populations (suspended and attached) were collected and washed twice with PBS. The cells were then stained with Annexin-V-fluorescein isothiocyanate-conjugated/propidium iodide (PI) reagents (Invitrogen, Carlsbad, CA, USA) to detect phosphatidylserine (PS) externalization for 15 min. Fluorescence-activated cell sorting was performed on a FACScalibur flow cytometer (Becton–Dickinson, Franklin Park, NJ, USA) to discriminate viable cells ($\text{Annexin-V}^-/\text{PI}^-$) from cells in early apoptosis ($\text{Annexin-V}^+/\text{PI}^-$), late apoptosis ($\text{Annexin-V}^+/\text{PI}^+$), or undergoing necrosis ($\text{Annexin-V}^-/\text{PI}^+$). Data analyses were performed with Cell Quest software (Becton–Dickinson). Non-treated culture cells were used as a negative control. U87 cells treated with 0.5 μM staurosporine (STS) were used as positive control.

4.3.1.4. Hemolysis assay. The hemolytic activity of tyrosol (1) and its derivatives was tested using human erythrocytes from healthy volunteers who had not taken any medication for at least 2 weeks prior to sampling. Freshly collected blood samples were immediately mixed with heparin. To obtain a pure suspension of erythrocytes, 1 mL of whole blood transferred to 20 mL PBS (pH 7.4) and centrifuged at 250g for 5 min at 4 °C. The supernatant and buffy coats were removed by gentle aspiration and the transfer/centrifugation process was repeated two more times. Erythrocytes were finally re-suspended in PBS to make a 1% solution for hemolytic assay. Various concentrations of tyrosol (1) and its novel derivatives were then added to the suspension of red blood cells and incubated at 37 °C for 1 h in a water bath, followed by centrifugation at 250g for 5 min at 4 °C. The absorbance of the supernatants was measured at 545 nm to determine the extent of red blood cell lysis. Positive (100% hemolysis) and negative (0% hemolysis) controls were generated by incubating erythrocytes in PBS containing 1% Triton X-100 and PBS alone, respectively [46]. All tests were performed in triplicate.

4.3.1.5. Statistical analysis. Statistical analysis was performed using Graph Pad Prism 7.0 (Graph Pad Software Inc., CA, and USA). All the data are presented as the mean \pm standard error of the mean (SEM). The difference between two groups was evaluated using Student's *t* test. Significant difference among three or more groups was determined by one-way ANOVA with a post hoc analysis (Turkey test). The values of $p < 0.05$, $p < 0.01$ and $p < 0.001$ were considered as statistically significant (*), very significant (**), highly significant difference (***) respectively, unless otherwise mentioned.

Declaration of Competing Interest

The authors declare that they have no known competing financial interests or personal relationships that could have appeared to influence the work reported in this paper.

Acknowledgments

We thank Pr. José Luis from Laboratory of Cell Biology, Faculty of Pharmacy, Marseille, France, for the kind gift of the human glioblastoma cells (U87) cells. Also, the authors are grateful to Researchers Supporting Project number (RSP-2021/17) at King Saud University, Riyadh, Saudi Arabia.

Funding

The authors are grateful to the Ministry of Higher Education and Scientific Research of Tunisia for financial support (LR11ES39).

Appendix A. Supplementary data

Supplementary data to this article can be found online at <https://doi.org/10.1016/j.bioorg.2021.105071>.

References

- H.B. Jannet, Z. Mighri, L. Serani, O. Laprevote, J.-C. Jullian, F. Roblot, Isolation and Structure Elucidation of Three New Diglyceride Compounds from *Ajuga Iva* Leaves, *Nat. Prod. Lett.* 10 (1997) 157–164.
- K. Chouaib, A. Romdhane, S. Delemasure, P. Dutartre, N. Elie, D. Touboul, H. Ben jannet, M. Ali Hamza, Regiospecific synthesis, anti-inflammatory and anticancer evaluation of novel 3,5-disubstituted isoxazoles from the natural maslinic and oleanolic acids, *Ind. Crops Prod.* 85 (2016) 287–299.
- K. Bozorov, J. Zhao, H.A. Aisa, 1,2,3-Triazole-containing hybrids as leads in medicinal chemistry: A recent overview, *Bioorg. Med. Chem.* 27 (2019) 3511–3531.
- J. Zhu, J. Mo, H. Lin, Y. Chen, H. Sun, The recent progress of isoxazole in medicinal chemistry, *Bioorg. Med. Chem.* 26 (2018) 3065–3075.
- N. Agrawal, P. Mishra, The synthetic and therapeutic expedition of isoxazole and its analogs, *Med. Chem. Res.* 27 (2018) 1309–1344.
- [https://clinicaltrials.gov/ct2/results?cond=&term=NVP-AUY922&cntry=\(n.d.\)](https://clinicaltrials.gov/ct2/results?cond=&term=NVP-AUY922&cntry=(n.d.)).
- M. Abbasi, H. Sadeghi-Aliabadi, M. Amanlou, Prediction of new Hsp90 inhibitors based on 3,4-isoxazolidinamide scaffold using QSAR study, molecular docking and molecular dynamic simulation, *DARU J. Pharm. Sci.* 25 (2017) 17.
- H. Wang, Y. Ma, Y. Lin, J. Liu, R. Chen, B. Xu, Y. Liang, An Isoxazole Derivative SHU00238 Suppresses Colorectal Cancer Growth through miRNAs Regulation, *Molecules* 24 (2019) 2335.
- X.-L. Wang, K. Wan, C.-H. Zhou, Synthesis of novel sulfanilamide-derived 1,2,3-triazoles and their evaluation for antibacterial and antifungal activities, *Eur. J. Med. Chem.* 45 (2010) 4631–4639.
- P. Suman, T.R. Murthy, K. Rajkumar, D. Srikanth, Ch. Dayakar, C. Kishor, A. Addlagatta, S.V. Kalivendi, B.C. Raju, Synthesis and structure-activity relationships of pyridinyl-1H-1,2,3-triazolyldihydroisoxazoles as potent inhibitors of tubulin polymerization, *Eur. J. Med. Chem.* 90 (2015) 603–619.
- E.T. Warda, I.A. Shehata, M.B. El-Ashmawy, N.S. El-Gohary, New series of isoxazole derivatives targeting EGFR-TK: Synthesis, molecular modeling and antitumor evaluation, *Bioorg. Med. Chem.* 28 (2020), 115674.
- D. Dheer, V. Singh, R. Shankar, Medicinal attributes of 1,2,3-triazoles: Current developments, *Bioorg. Chem.* 71 (2017) 30–54.
- K. Chouaib, S. Delemasure, P. Dutartre, H.B. Jannet, Microwave-assisted synthesis, anti-inflammatory and anti-proliferative activities of new maslinic acid derivatives bearing 1,5- and 1,4-disubstituted triazoles, *J. Enzyme Inhib. Med. Chem.* 31 (2016) 130–147.
- J. Mareddy, N. Suresh, C.G. Kumar, R. Kapavarapu, A. Jayasree, S. Pal, 1,2,3-Triazole-nimesulide hybrid: Their design, synthesis and evaluation as potential anticancer agents, *Bioorg. Med. Chem. Lett.* 27 (2017) 518–523.
- Z. Xu, S.-J. Zhao, Y. Liu, 1,2,3-Triazole-containing hybrids as potential anticancer agents: Current developments, action mechanisms and structure-activity relationships, *Eur. J. Med. Chem.* 183 (2019), 111700.
- S. Balabadra, M. Kotni, V. Manga, A.D. Allanki, R. Prasad, P.S. Sijwali, Synthesis and evaluation of naphthyl bearing 1,2,3-triazole analogs as antiplasmodial agents, cytotoxicity and docking studies, *Bioorg. Med. Chem.* 25 (2017) 221–232.
- K. Lal, P. Yadav, A. Kumar, A. Kumar, A.K. Paul, Design, synthesis, characterization, antimicrobial evaluation and molecular modeling studies of some dehydroacetic acid-chalcone-1,2,3-triazole hybrids, *Bioorg. Chem.* 77 (2018) 236–244.
- P. Sooknual, R. Pingaew, K. Phopin, W. Ruankham, S. Prachayasittikul, S. Ruchirawat, V. Prachayasittikul, Synthesis and neuroprotective effects of novel chalcone-triazole hybrids, *Bioorg. Chem.* 105 (2020), 104384.
- J. Akhtar, A.A. Khan, Z. Ali, R. Haider, M. Shahar Yar, Structure-activity relationship (SAR) study and design strategies of nitrogen-containing heterocyclic moieties for their anticancer activities, *Eur. J. Med. Chem.* 125 (2017) 143–189.
- V.D. da Silva, B.M. de Faria, E. Colombo, L. Ascari, G.P.A. Freitas, L.S. Flores, Y. Cordeiro, L. Romão, C.D. Buarque, Design, synthesis, structural characterization and in vitro evaluation of new 1,4-disubstituted-1,2,3-triazole derivatives against glioblastoma cells, *Bioorg. Chem.* 83 (2019) 87–97.
- A. Ogino, E. Sano, Y. Ochiai, S. Yamamoto, T. Ueda, A. Yoshino, Y. Katayama, Efficacy of ribavirin against malignant glioma cell lines, *Oncol. Lett.* 8 (2014) 2469–2474.
- I. Lampronti, D. Simoni, R. Rondanin, R. Baruchello, C. Scapoli, A. Finotti, M. Borgatti, C. Tupini, R. Gambari, Pro-apoptotic activity of novel synthetic isoxazole derivatives exhibiting inhibitory activity against tumor cell growth *in vitro*, *Oncol. Lett.* 20 (2020) 151.
- Y.J. Rao, T. Sowjanya, G. Thirupathi, N.Y.S. Murthy, S.S. Kotapalli, Synthesis and biological evaluation of novel flavone/triazole/benzimidazole hybrids and flavone/isoxazole-annulated heterocycles as antiproliferative and antimycobacterial agents, *Mol. Divers.* 22 (2018) 803–814.
- T. Sowjanya, Y. Jayaprakash Rao, N.Y.S. Murthy, Synthesis and antiproliferative activity of new 1,2,3-triazole/flavone hybrid heterocycles against human cancer cell lines, *Russ. J. Gen. Chem.* 87 (2017) 1864–1871.
- S. Chekir, M. Debbabi, A. Regazzetti, D. Dargère, O. Laprevote, H. Ben Jannet, R. Gharbi, Design, synthesis and biological evaluation of novel 1,2,3-triazole linked coumarinopyrazole conjugates as potent anticholinesterase, anti-5-lipoxygenase, anti-tyrosinase and anti-cancer agents, *Bioorg. Chem.* 80 (2018) 189–194.
- A. Bistrovic, N. Stipanicev, T. Opačak-Bernardi, M. Jukić, S. Martinez, Lj. Glavaš-Obrovac, S. Raić-Malić, Synthesis of 4-aryl-1,2,3-triazolyl appended natural coumarin-related compounds with antiproliferative and radical scavenging activities and intracellular ROS production modification, *New J. Chem.* 41 (2017) 7531–7543.
- Y. Qi, Z. Ding, Y. Yao, D. Ma, F. Ren, H. Yang, A. Chen, Novel triazole analogs of apigenin-7-methyl ether exhibit potent antitumor activity against ovarian carcinoma cells via the induction of mitochondrial-mediated apoptosis, *Exp. Ther. Med.* (2018).
- A. Karković Marković, J. Torić, M. Barbarić, C. Jakobušić Brala, Hydroxytyrosol, Tyrosol and Derivatives and Their Potential Effects on Human Health, *Molecules* 24 (2019) 2001.
- M.I. Fernández-Mar, R. Mateos, M.C. García-Parrilla, B. Puertas, E. Cantos-Villar, Bioactive compounds in wine: Resveratrol, hydroxytyrosol and melatonin: A review, *Food Chem.* 130 (2012) 797–813.
- Y. Zhang, Z. Zhou, L. Zou, R. Chi, Imidazolium-based ionic liquids with inorganic anions in the extraction of salidroside and tyrosol from *Rhodiola*: The role of cations and anions on the extraction mechanism, *J. Mol. Liq.* 275 (2019) 136–145.
- A. Chang, S. Sun, L. Li, X. Dai, H. Li, Q. He, H. Zhu, Tyrosol from marine Fungi, a novel Quorum sensing inhibitor against *Chromobacterium violaceum* and *Pseudomonas aeruginosa*, *Bioorg. Chem.* 91 (2019), 103140.

- [32] M.B. Plotnikov, O.I. Aliev, A.V. Sidekhenova, A.Y. Shamanaev, A. M. Anishchenko, T.I. Fomina, T.M. Plotnikova, A.M. Arkhipov, Effect of p-tyrosol on hemorheological parameters and cerebral capillary network in young spontaneously hypertensive rats, *Microvasc. Res.* 119 (2018) 91–97.
- [33] I. Aissa, M. Bouaziz, F. Frikha, R.B. Mansour, Y. Gargouri, Synthesized tyrosyl hydroxyphenylacetate, a novel antioxidant, anti-stress and antibacterial compound, *Process Biochem.* 47 (2012) 2356–2364.
- [34] E.-Y. Ahn, Y. Jiang, Y. Zhang, E. Son, S. You, S.-W. Kang, J.-S. Park, J. Jung, B.-J. Lee, D.-K. Kim, Cytotoxicity of p-tyrosol and its derivatives may correlate with the inhibition of DNA replication initiation, *Oncol. Rep.* 19 (2008) 527–534.
- [35] I. Aissa, R. Sghair, M. Bouaziz, D. Laouini, S. Sayadi, Y. Gargouri, Synthesis of lipophilic tyrosyl esters derivatives and assessment of their antimicrobial and antileishmania activities, *Lipids Health Dis.* 11 (2012) 13.
- [36] F. Himo, T. Lovell, R. Hilgraf, V.V. Rostovtsev, L. Noodleman, K.B. Sharpless, V. V. Fokin, Copper(I)-Catalyzed Synthesis of Azoles. DFT Study Predicts Unprecedented Reactivity and Intermediates, *J. Am. Chem. Soc.* 127 (2005) 210–216.
- [37] R. Naresh Kumar, G. Jitender Dev, N. Ravikumar, D. Krishna Swaroop, B. Debanjan, G. Bharath, B. Narsaiah, S. Nishant Jain, A. Gangagni Rao, Synthesis of novel triazole/isoxazole functionalized 7-(trifluoromethyl)pyrido[2,3-*d*]pyrimidine derivatives as promising anticancer and antibacterial agents, *Bioorg. Med. Chem. Lett.* 26 (2016) 2927–2930.
- [38] G. Wei, W. Luan, S. Wang, S. Cui, F. Li, Y. Liu, Y. Liu, M. Cheng, A library of 1,2,3-triazole-substituted oleanolic acid derivatives as anticancer agents: design, synthesis, and biological evaluation, *Org. Biomol. Chem.* 13 (2015) 1507–1514.
- [39] D. Kumar, V.B. Reddy, R.S. Varma, A facile and regioselective synthesis of 1,4-disubstituted 1,2,3-triazoles using click chemistry, *Tetrahedron Lett.* 50 (2009) 2065–2068.
- [40] L.-J. Li, Y.-Q. Zhang, Y. Zhang, A.-L. Zhu, G.-S. Zhang, Synthesis of 5-functionalized-1,2,3-triazoles via a one-pot aerobic oxidative coupling reaction of alkynes and azides, *Chin. Chem. Lett.* 25 (2014) 1161–1164.
- [41] P. Das, M.H. Hasan, D. Mitra, R. Bollavarapu, E.J. Valente, R. Tandon, D. Raucher, A.T. Hamme, Design, Synthesis, and Preliminary Studies of Spiro-isoxazoline-peroxides against Human Cytomegalovirus and Glioblastoma, *J. Org. Chem.* 84 (2019) 6992–7006.
- [42] M. Khazaei, M. Pazhouhi, S. Khazaei, Temozolomide and tranilast synergistic antiproliferative effect on human glioblastoma multiforme cell line (U87MG), *Med. J. Islam. Republ. Iran* 33 (2019) 39.
- [43] M. Allam, A.K.D. Bhavani, A. Mudiraj, N. Ranjan, M. Thippana, P.P. Babu, Synthesis of pyrazolo[3,4-*d*]pyrimidin-4(5H)-ones tethered to 1,2,3-triazoles and their evaluation as potential anticancer agents, *Eur. J. Med. Chem.* 156 (2018) 43–52.
- [44] G. Jeswani, A. Alexander, S. Saraf, S. Saraf, A. Qureshi, Ajazuddin, Recent approaches for reducing hemolytic activity of chemotherapeutic agents, *J. Controlled Release* 211 (2015) 10–21.
- [45] T. Mosmann, Rapid colorimetric assay for cellular growth and survival: Application to proliferation and cytotoxicity assays, *J. Immunol. Methods* 65 (1983) 55–63.
- [46] M. Malagoli, A full-length protocol to test hemolytic activity of palytoxin on human erythrocytes, *Invertebr. Surviv. J.* 4 (2007) 92–94.